



# Thermophysical properties of KCl-NaF reciprocal eutectic by artificial neural network prediction and experimental measurements

Yang Wang<sup>a,b</sup>, Changjian Ling<sup>a,c,d</sup>, Huiqin Yin<sup>a,c,d</sup>, Weihua Liu<sup>a,c,d</sup>, Zhongfeng Tang (Ph.D)<sup>a,b,c,d,\*</sup>, Zhong Li (Ph.D)<sup>a,\*</sup>

<sup>a</sup> Shanghai Institute of Applied Physics, Chinese Academy of Sciences, Shanghai 201800, China

<sup>b</sup> University of Chinese Academy of Sciences, Beijing 100049, China

<sup>c</sup> Key Laboratory of Interfacial Physics and Technology, Chinese Academy of Sciences, Shanghai 201800, China

<sup>d</sup> Dalian National Laboratory for Clean Energy, Dalian 116023, China

## ARTICLE INFO

### Keywords:

Phase change material (PCM)  
 Molten salt  
 Thermal energy storage (TES)  
 Artificial neural network (ANN)  
 Thermophysical property

## ABSTRACT

Fluoride and chloride reciprocal salts are potential novel media with suitable working temperature and high latent heat for next-generation solar power. A back propagation (BP) artificial neural network (ANN) algorithm was developed based on the known data of salts. The composition and melting point of two unknown binary fluoride and chloride reciprocal salts were predicted by the trained ANN model. The predicted composition and melting point of the reciprocal salts were verified by experimental tests. The predicted results of composition are in good agreement with the experimental values, and the predicted errors of the melting point are less than 1.5%. The melting point and fusion enthalpy of KCl-NaF reciprocal eutectic salt are  $648 \pm 2$  °C and  $365 \pm 5$  J/g, respectively. The thermal stability of this reciprocal eutectic salt is very good and the weight loss is still less than 3.0% even up to 800 °C. The good performance of KCl-NaF reciprocal eutectic salt at high temperatures suggest that it can be a good candidate for thermal energy storage systems with supercritical CO<sub>2</sub> cycles. The ANN is an effective method to prediction composition and properties of molten salts, this method is expected to a quick method for design and selection of phase change material for the high temperature latent heat energy storage systems.

## 1. Introduction

Nitrate salts are commonly applied as thermal energy storage mediums for large-scale concentrating solar power (CSP) plants at present due to their low cost and large heat capacity (Reilly and Kolb, 2001; Herrmann and Kearney, 2002). However, their upper temperature limit of 565 °C (Stern, 1972; Hoshino et al., 1981) make the economy of CSP still difficult to match with traditional fossil fuel-based power (Fernández et al., 2019; Mohan et al., 2019). High temperature phase change materials (PCM) have gained increasing interest for thermal energy storage (TES) (Kenisarin, 2010; Myers and Goswami, 2016; Lin et al., 2018; Zhou and Wu 2019). High temperature PCM not only reduce the cost of TES systems but also allow the systems to be integrated with more efficient power generation systems, such as supercritical CO<sub>2</sub> (S-CO<sub>2</sub>) cycles (Jiang et al., 2018).

The development of high-temperature PCM has focused on PCM composite with nanoparticles (Navarrete et al., 2019; Xiao et al., 2019), skeleton/supporting materials (Li et al., 2019; Sang et al., 2019) or

encapsulated PCMs (Zou et al., 2019; Zhang et al., 2019) to overcome the low specific heat and (or) thermal conductivity of salts. There are rare studies on high temperature molten salt PCMs itself with high latent heat and suitable temperature. Fluoride and chloride eutectic salt has the highest latent heat and satisfies the temperature requirement (600–720 °C) for higher efficiency next-generation CSP (Kenisarin, 2010; Myers and Goswami, 2016; Mohan et al., 2019; Zhou and Wu 2019). Although some fluoride and chloride reciprocal eutectic salts have been investigated recently, most of these studies focused on phase behavior (Chartrand and Pelton, 2001; Pelton et al., 1992; Renaud et al., 2011). Few experimental investigations on thermal storage behavior are available. Verdiev et al. (2006, 2009) evaluated fusion enthalpy ( $\Delta H$ ) and melting temperature ( $T_m$ ) of NaF-NaCl (33.5–66.5 mol%) and KF-KCl (55.0–45.0 mol%). The  $T_m$  of NaF-NaCl and KF-KCl were 675 °C and 605 °C, respectively. The corresponding  $\Delta H$  were 572 J/g and 407 J/g, respectively. These results indicate that the fluoride and chloride reciprocal system is an appropriate high latent candidate PCM for TES. Researchers (Cheng and Zhai,

\* Corresponding authors at: P.O. Box 800-204, Shanghai 201800, China (Z. Tang).

E-mail addresses: [tangzhongfeng@sinap.ac.cn](mailto:tangzhongfeng@sinap.ac.cn) (Z. Tang), [lizhong@sinap.ac.cn](mailto:lizhong@sinap.ac.cn) (Z. Li).

<https://doi.org/10.1016/j.solener.2020.05.029>

Received 10 February 2020; Received in revised form 7 May 2020; Accepted 10 May 2020

Available online 19 May 2020

0038-092X/© 2020 International Solar Energy Society. Published by Elsevier Ltd. All rights reserved.

2018; Elfeky et al., 2019) studied the thermal performance of multi-layered PCM with different  $T_m$  configurations and compared the outcomes with those of a single-stage PCM configuration. The multilayered PCM configuration has the better performance and can reduce the charging time by up to 15.1% relative to those of a single-stage PCM. Developing more fluoride and chloride reciprocal eutectic salts with different melting points is necessary for multilayered PCM configuration.

An artificial neural network (ANN) algorithm is a machine learning technology that uses samples with known data as the training set to establish a model and then predict the properties of unknown samples. The machine learning has been applied in biomedicine and chemical synthesis (Coley et al., 2019; Zhavoronkov et al., 2019), chemical substance characterizations (Gadzuric et al., 2006; Liu, et al., 2016; Isayev, et al. 2017) and phase diagram analysis of an alloy (Zeng et al., 1997; Zhu et al. 2018). Therefore, ANN method may be applicable to predict the characteristics of new molten salts without experimental tests. A back propagation (BP) ANN algorithm was established using the binary fluoride/chloride reciprocal salts with known composition data and  $T_m$  as the test set from the literature. The compositions and  $T_m$  value of two unknown binary fluoride and chloride reciprocal salts were predicted by the trained model. The Differential Scanning Calorimeter (DSC) tests confirmed the accuracy of the predicted results. The key thermophysical properties of KCl-NaF reciprocal eutectic salt were achieved by experiments. The suitable phase change temperature, high latent heat and good thermal stability of KCl-NaF reciprocal eutectic salt make it be a good candidate for next-generation CSP. ANN method could be further developed for predicting composition and melting points of multi-component molten salts, and also for ascertaining the other properties of molten salts, such as their densities, conductivities and so on. This ANN method is expected to provide a quick technique for molten salt design, selection of PCM for latent heat energy storage systems at high temperature.

## 2. Materials and methods

### 2.1. ANN calculation

ANN method is one of the machine learning algorithms that adopt samples of known data as the training set to establish a prediction model and then predict the properties of unknown samples. A three-layer back propagation ANN used in the study contains input layer, hidden layer, and output layer. The sketch map of ANN was shown in Fig. 1. The mean square error (MSE) function (1) was employed as the loss function, and the sigmoid function (2) was applied as activation function. Learning rate decay and momentum were added into the ANN to improve the BP neural network algorithm and overcome the problems of local minimum and slow convergence. The alkali or alkaline earth fluoride and chloride reciprocal salts with known compositions and  $T_m$  values were applied as the training set. Molecular and atomic parameters were selected as the descriptors (input). The lowest  $T_m$

value and composition of the eutectic salt were set as the outputs. The calculation accuracies of the ANN algorithm were verified by the leave-one-out cross-validation method. Unknown salts that were the subject to prediction were taken as the test set.

$$\text{MSE loss function, } MSE = \frac{1}{n} \sum_{i=1}^n (y_i - t_i)^2 \quad (1)$$

$$\text{Activation function, } f(x) = \frac{1}{1 + e^x} \quad (2)$$

### 2.2. Molten salt preparation

Individual salts of KCl, NaF and  $MgF_2$  were purchased from Sinopharm Chemical Regent Co., Ltd and their purities were more than 99.8%. The individual salts were weighed by balance according to the eutectic composition by prediction or the given comparison composition. The raw materials were putted into quartz crucibles and then heated to 680 °C or 800 °C, at which they were maintained for 50 min. A rod was utilized to stir the salts when kept at 680 °C or 800 °C for adequately mix the salts. The mixtures were cooled naturally and finally preserved in glove box for following experiments.

### 2.3. Characterization

The  $T_m$  value and fusion enthalpy were measured by the NETZSCH DSC (DSC-404 F3). The samples were first ground to powders, and then approximately 10.0 mg of powders were added into the test pan. The samples were heated from ambient temperature to 800 °C with the scanning rate of 5.0 °C·min<sup>-1</sup>. The experiment was conducted under argon atmosphere and the flow rate of purge gas is 50.0 ml·min<sup>-1</sup>. The heat and cool processes for each sample were repeated three times to ensure reproducibility of results.

Thermal stability of eutectic salt was evaluated by a thermogravimetric analyzer (TGA, Setaram Labsys Evo). TGA test was performed under argon atmosphere from 300 °C to 900 °C at a heating speed of 10.0 °C·min<sup>-1</sup>. During measurement, the test corundum crucible was first heated to 900 °C as the baseline of the result. Approximately 30 mg of the reciprocal eutectic salt was added into the crucible and heated to 900 °C under the same condition as the baseline test. The baseline was subtracted from the weight change of experiment result.

## 3. Results and discussion

### 3.1. Composition and melting point prediction

The composition and melting temperature can be usually obtained through Calculation of phase diagram (Calphad) software such as Factsage, the calculation of Calphad software based on a large number of experimental phase equilibrium data and thermochemical data. It can only evaluating ternary molten system from binary molten system

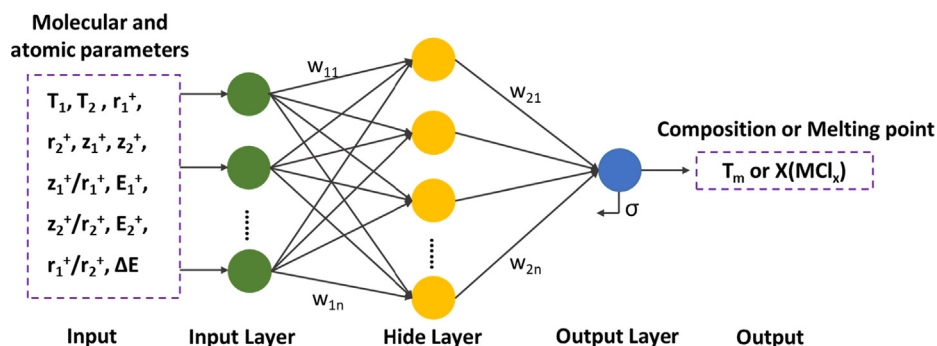


Fig. 1. The sketch map of the ANN model.

or optimize binary phase diagram based on experimental data of corresponding molten system. The experimental phase equilibrium data and thermochemical data of the fluoride/chloride reciprocal salt are incomplete and very difficult to acquire by experiments. Research on phase behavior of fluoride/chloride reciprocal salt by traditional method is highly complex and time consuming. In particular, for the binary salt, the composition and diagram should be obtained totally based on experimental tests and cannot be calculated only by the phase diagram thermodynamic method. ANN method can predict the properties of unknown molten systems based on molten systems with existing data, it can avoid do experiment test on the unknown molten system and consider the intermediate compound, especially suited for high temperature and (or) danger systems.

The eutectic composition and  $T_m$  of KCl-NaF reciprocal salt has been investigated by the ANN method. The KCl-MgF<sub>2</sub> reciprocal salt was also predicted to further verify the reliability of the ANN algorithm. These two reciprocal salts were taken as the test set. A total of 23 samples of alkali or alkaline earth chloride/fluoride reciprocal salts with eutectic compositions and  $T_m$  values were obtained from the literature and served as the training set. The lowest eutectic composition (shown here as a component of chloride,  $X(MCl_x)$ ) and the  $T_m$  of these reciprocal salts are shown in Table 1. Molecular and atomic parameters were usually chosen as the descriptors (input) in data mining or machine learning in chemistry (Gadzuric et al., 2006; Liu, et al., 2016; Isayev, et al. 2017; Zeng et al., 1997). The descriptors selected in the paper include cation radius (r), electronegativity (E), electronegativity difference ( $\Delta E$ ), cationic charge (Z), and cationic charge/radius ratio (Z/r). The  $T_m$  of individual salts were also selected as descriptors. Subscripts 1 and 2 are representations of chloride and fluoride, respectively. The parameters of these molten salts were collected from the references (Songster and Pelton, 1991; Sharma and Johnson, 1969; Malinovský and Gregorčoková, 1974; Janz et al., 1979; Pelton et al., 1992; Chartrand and Pelton, 2001; Renaud et al., 2011; Garkushin et al., 2017). Allred-Rochow electronegativity (You, 1974) was applied as a descriptor to enlarge the difference in the electronegativity among different elements. The detailed descriptor parameters and their values are presented in Table 1. The  $X(MCl_x)$  and  $T_m$  of eutectic salts were set as the outputs. The accuracies of the ANN algorithm were verified by the leave-one-out cross-validation method because of the dataset is

small. Fig. 2 shows the cross-validation results of the predicted against the experimental values of eutectic compositions and  $T_m$  values, respectively. The prediction errors of most samples were within the  $\pm 10\%$  range, and the  $R^2$  values of the composition and  $T_m$  were 91.10% and 86.88%, respectively. These results indicated a high precision and confidence for the predictions.

After cross-validation, the ANN was trained by utilizing the 23 samples of molten salts with known compositions and  $T_m$  as the training set, the selected descriptors as inputs, and  $X(MCl_x)$  or  $T_m$  as outputs. The descriptors of KCl-NaF and KCl-MgF<sub>2</sub> reciprocal eutectic salts were inputted to the trained ANN. Compositions and  $T_m$  were predicted by the established models. The predicted content of KCl for KCl-NaF and KCl-MgF<sub>2</sub> reciprocal eutectic salts were 72.8% and 94.2%, and the  $T_m$  values were 652.6 °C and 776.6 °C, respectively. The reciprocal salts with the predicted composition were prepared, and their DSC curves were tested to validate the reliability of calculation. The experimental results of the KCl-NaF and KCl-MgF<sub>2</sub> reciprocal eutectic salts are shown in Fig. 3. Only one peak was found for each reciprocal salt with the predicted composition. The  $T_m$  values of KCl-NaF and KCl-MgF<sub>2</sub> reciprocal eutectic salts by the DSC test were 649.5 °C and 766.2 °C, respectively. The peak locations were in good agreement with the predicted values, and the predicted errors of  $T_m$  values were less than 1.5%. The relationship of predicted against experimental values for eutectic composition and  $T_m$  are also reflected in Fig. 2 by blue stars.

### 3.2. Composition and melting point validation

The accuracy of the ANN prediction results was further validated by the DSC test of salts with different compositions. For the KCl-NaF system, besides the salt at the composition of the predicted eutectic point, five other salts with KCl contents of 90.0, 80.0, 70.0, 60.0, and 50.0 mol% were analyzed by DSC. The DSC test results of these salts are provided in Fig. 4. Fig. 4(a) and (b) shows the DSC curves of the heat up and cool down process, respectively. Two peaks were found in all of these salt samples, except for the salt with a predicted composition in Fig. 4. The first peaks were at a constant temperature of approximately 647.3–649.5 °C. This temperature range is the lowest  $T_m$  of the KCl-NaF reciprocal salt. The location of the second peak changed with the composition, that is, the bigger the gap between the composition of the

**Table 1**  
The composition, melting point and value of descriptors of training set (23 samples) and test set (2 samples).

No.	Eutectic	$T_m$	$X(MCl_x)$	$T_1$	$T_2$	$r_1^+$	$r_2^+$	$z_1^+$	$z_2^+$	$z/r_1^+$	$z/r_2^+$	$r_1^+/r_2^+$	$E_1^+$	$E_2^+$	$\Delta E$	Ref.
1	NaCl-CaF <sub>2</sub>	779	0.955	801	1418	0.95	0.99	1	2	1.0526	2.0202	0.9596	7.21	8.58	-1.37	Malinovský and Gregorčoková (1974)
2	KCl-CaF <sub>2</sub>	763	0.984	771	1418	1.33	0.99	1	2	0.7519	2.0202	1.3434	4.17	8.58	-4.41	Chartrand and Pelton (2001)
3	NaCl-MgF <sub>2</sub>	786	0.955	801	1263	0.95	0.65	1	2	1.0526	3.0769	1.4615	7.21	17.80	-10.59	Sharma and Johnson (1969)
4	LiCl-CaF <sub>2</sub>	495	0.813	605	1418	0.60	0.99	1	2	1.6667	2.0202	0.6061	6.67	8.58	-1.91	Chartrand and Pelton (2001)
5	LiCl-MgF <sub>2</sub>	597	0.980	605	1263	0.60	0.65	1	2	1.6667	3.0769	0.9231	6.67	17.80	-11.13	Chartrand and Pelton (2001)
6	LiCl-SrF <sub>2</sub>	492	0.875	605	1477	0.60	1.13	1	2	1.6667	1.7699	0.5310	6.67	7.75	-1.08	Renaud et al. (2011)
7	NaCl-SrF <sub>2</sub>	757	0.919	801	1477	0.95	1.13	1	2	1.0526	1.7699	0.8407	7.21	7.75	-0.54	Renaud et al. (2011)
8	KCl-SrF <sub>2</sub>	760	0.985	771	1477	1.33	1.13	1	2	0.7519	1.7699	1.1770	4.17	7.75	-3.58	Renaud et al. (2011)
9	KCl-BaF <sub>2</sub>	739	0.924	771	1368	1.33	1.35	1	2	0.7519	1.4815	0.9852	4.17	5.43	-1.26	Janz et al. (1979)
10	NaCl-NaF	679	0.665	801	995	0.95	0.95	1	1	1.0526	1.0526	1.0000	7.21	7.21	0.00	Chartrand and Pelton (2001)
11	MgCl <sub>2</sub> -MgF <sub>2</sub>	627	0.772	714	1263	0.65	0.65	2	2	3.0769	3.0769	1.0000	17.80	17.80	0.00	Pelton et al. (1992)
12	KCl-KF	605	0.550	771	858	1.33	1.33	1	1	0.7519	0.7519	1.0000	4.17	4.17	0.00	Chartrand and Pelton (2001)
13	CaCl <sub>2</sub> -CaF <sub>2</sub>	645	0.819	775	1418	0.99	0.99	2	2	2.0202	2.0202	1.0000	8.58	8.58	0.00	Pelton et al. (1992)
14	LiCl-LiF	485	0.680	605	848	0.60	0.60	1	1	1.6667	1.6667	1.0000	6.67	6.67	0.00	Janz et al. (1979)
15	CaCl <sub>2</sub> -MgF <sub>2</sub>	695	0.875	775	1263	0.99	0.65	2	2	2.0202	3.0769	1.5231	8.58	17.80	-9.22	Pelton et al. (1992)
16	NaCl-LiF	681	0.578	801	848	0.95	0.60	1	1	1.0526	1.6667	1.5833	7.21	6.67	0.54	Chartrand and Pelton (2001)
17	KCl-LiF	718	0.780	771	848	1.33	0.60	1	1	0.7519	1.6667	2.2167	4.17	6.67	-2.5	Chartrand and Pelton (2001)
18	RbCl-RbF	540	0.540	718	775	1.48	1.48	1	1	0.6757	0.6757	1.0000	4.07	4.07	0.00	Janz et al. (1979)
19	SrCl <sub>2</sub> -SrF <sub>2</sub>	740	0.880	874	1477	1.13	1.13	2	2	1.7699	1.7699	1.0000	7.75	7.75	0.00	Renaud et al. (2011)
20	CsCl-CsF	430	0.500	645	682	1.69	1.69	1	1	0.5917	0.5917	1.0000	3.12	3.12	0.00	Songster and Pelton (1991)
21	BaCl <sub>2</sub> -BaF <sub>2</sub>	845	0.827	963	1368	1.35	1.35	2	2	1.4815	1.4815	1.0000	5.43	5.43	0.00	Janz et al. (1979)
22	CsCl-KF	482	0.660	645	858	1.69	1.33	1	1	0.5917	0.7519	1.2707	3.12	4.17	-1.05	Garkushin et al. (2017)
23	CsCl-NaF	583	0.880	645	995	1.69	0.95	1	1	0.5917	1.0526	1.7789	3.12	7.21	-4.09	Garkushin et al. (2017)
Test1	KCl-NaF*	652.6	0.728	771	995	1.33	0.95	1	1	0.7519	1.0526	1.4000	4.17	7.21	-3.04	Test set
Test2	KCl-MgF <sub>2</sub> *	776.6	0.942	771	1263	1.33	0.65	1	2	0.7519	3.0769	0.9231	4.17	17.80	-13.63	Test set

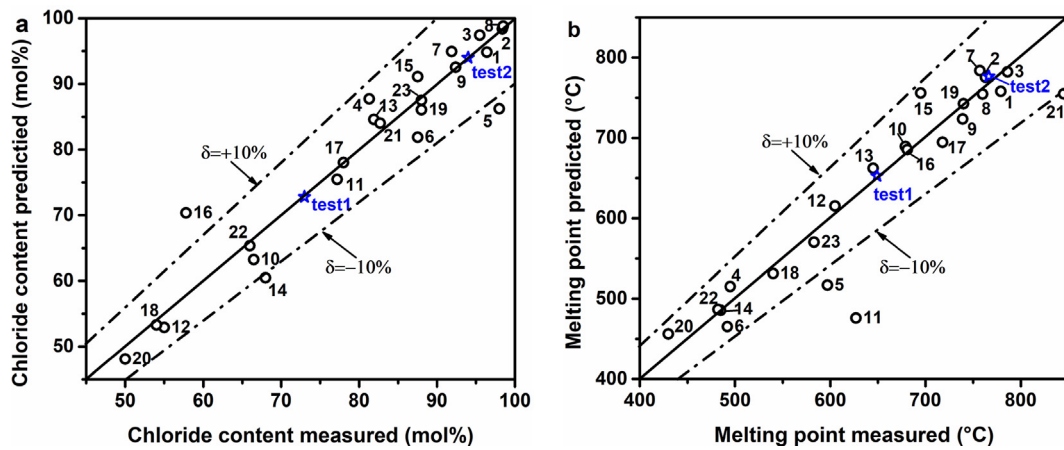


Fig. 2. Cross-validation of the predicted values of alkali or alkaline earth chloride or fluoride molten salts using the leave-one-out method: (a) composition of chloride ( $X(\text{MCl}_x)$ ) and (b) melting point ( $T_m$ ).

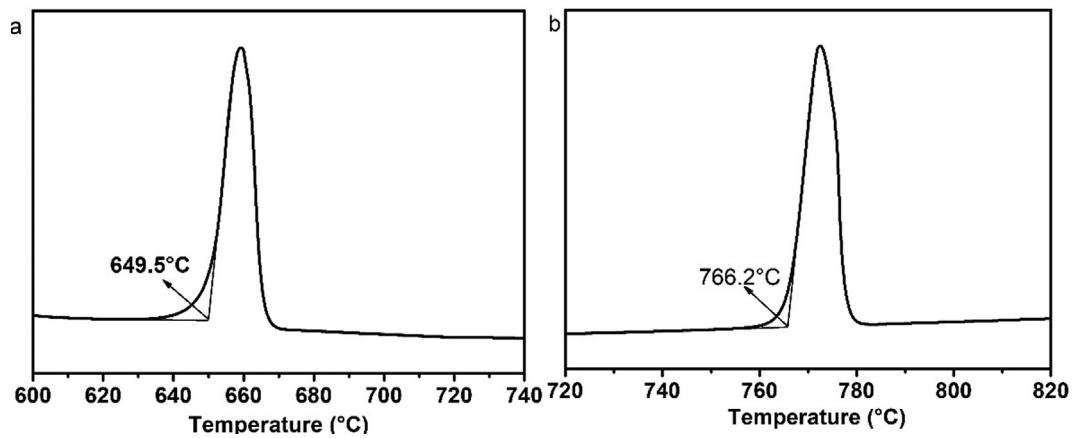


Fig. 3. DSC curves of reciprocal eutectic salt in test set: (a) KCl-NaF, (b) KCl-MgF<sub>2</sub>.

comparison salts and the ANN prediction value, the farther away the second peak is from the first one. Moreover, the second peak areas were also increase with the bigger of gaps. Only one peak started at approximately 649 °C for the salt with the predicted composition, and no other peaks were found at other temperatures (Fig. 4). This composition is the eutectic composition of KCl-NaF reciprocal salt or very close to it.

KCl-MgF<sub>2</sub> reciprocal salts with different compositions were also subjected to DSC tests for further validation (Fig. 5). The KCl-MgF<sub>2</sub> reciprocal salt with predicted composition had only one peak. Two peaks occurred in the DSC curves of the comparison salt whose composition deviated from the predicted value. The comparison salt is not a eutectic salt. These results indicate that the ANN prediction eutectic

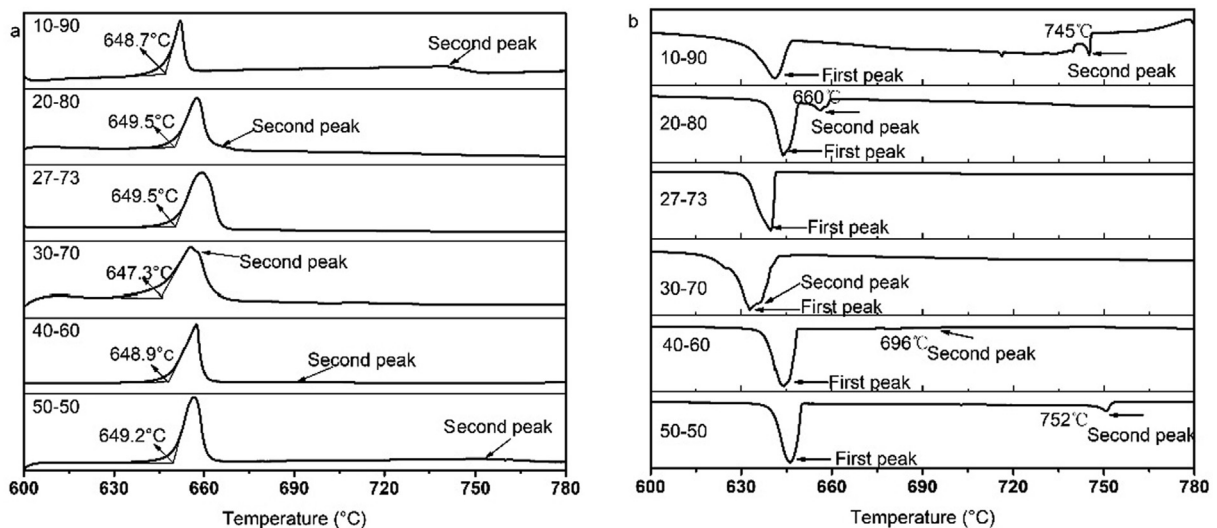


Fig. 4. The DSC curves of KCl-NaF reciprocal eutectic with different composition: (a) Heat up, (b) Cool down.

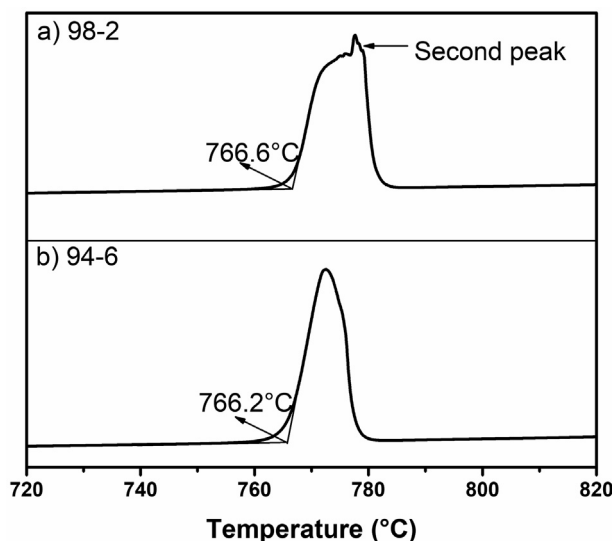


Fig. 5. The DSC curves of KCl-MgF<sub>2</sub> reciprocal salt with different composition: (a) 98–2 mol%; (b) 94–6 mol%.

point is the lowest one, and the calculation of the melting points is accurate. Thus, the ANN prediction is not only limited to one sample but is applicable to similar samples.

### 3.3. Key thermophysical properties

The  $T_m$  and enthalpy of fusion of the KCl-NaF reciprocal eutectic salts were measured by DSC (Fig. 6). The onset temperature of the peak in the DSC curve was taken as the  $T_m$  of this eutectic salt, which was  $648 \pm 2$  °C. Enthalpy of fusion is a key parameter for latent heat storage which was calculated by the integration of the peak area in the DSC curve. The fusion enthalpy of the KCl-NaF reciprocal eutectic salt was  $365 \pm 5$  J/g. The KCl-NaF reciprocal eutectic salt with suitable melting point and high latent heat may be a good candidate medium for next-generation solar power technology.

The TGA spectra of KCl-NaF reciprocal eutectic salt was shown in Fig. 7. The TGA of KCl-NaF reciprocal eutectic salt was conducted with the heating speed of  $5.0$  °C·min<sup>-1</sup> under argon atmosphere. There is not weight change from 300 °C to 700 °C for the KCl-NaF reciprocal eutectic salt (Fig. 7). The weight loss between 700 °C and 750 °C is slowly and less than 1.5 wt%. The weight loss is still less than 3.0 wt% even up to 800 °C. A weight loss of 3.0 wt% is usually regarded as the thermal decomposition (degradation) temperature (Fernández et al., 2019). Therefore, KCl-NaF reciprocal eutectic salt has good thermal stability,

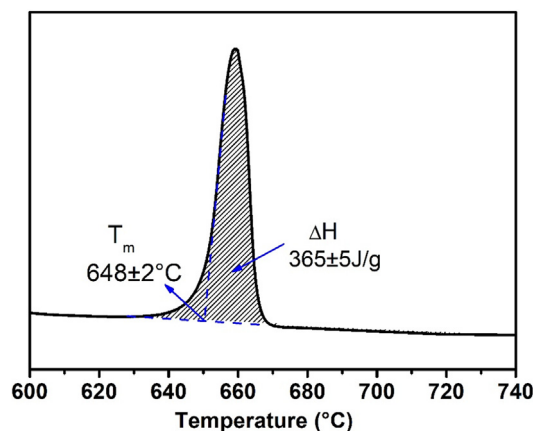


Fig. 6. The melting point ( $T_m$ ) and enthalpy of fusion ( $\Delta H$ ) of KCl-NaF reciprocal eutectic salt.

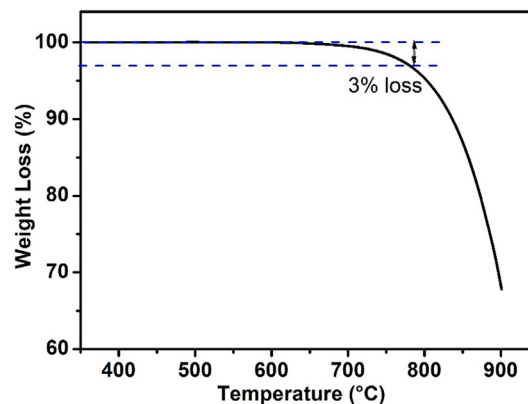


Fig. 7. TGA spectra of KCl-NaF reciprocal eutectic salt.

which determined the upper limit of the working temperature. The good thermal stability of KCl-NaF eutectic salt at high temperatures indicated that it can fulfill the temperature requirement for the TES systems with S-CO<sub>2</sub> power-generation cycles.

## 4. Conclusions

An ANN algorithm was developed based on molecular and atomic parameters of known eutectic salts. Eutectic compositions and melting point of binary fluoride and chloride reciprocal eutectic salts were predicted by the trained ANN model. The predicted composition and melting point of the reciprocal salts were verified by experimental tests. The single peak in the Differential Scanning Calorimeter curves indicates the high accuracy of the predicted values for the reciprocal salts, and the predicted errors of the melting point are less than 1.5%. The predicted compositions and melting point are in good agreement with the experimental values. The melting temperature and fusion enthalpy of KCl-NaF reciprocal eutectic salt are  $648 \pm 2$  °C and  $365 \pm 5$  J/g, respectively. The thermal stability of this reciprocal eutectic salt is very good and the weight loss is still less than 3.0% even up to 800 °C. The KCl-NaF reciprocal eutectic salt with satisfactory thermophysical properties at high temperatures could be a good candidate medium for next-generation solar power technology. The ANN is an effective method to prediction composition and melting points of binary molten salts. It can avoid to do experiment test on the unknown molten system and consider the intermediate compound, especially suited for high temperature and (or) danger systems. The Calphad software, such as Factsage, can apply for more complicated salts and more thermophysical properties. As a novel and immaturity algorithm, the ANN method may and should also be further developed for predicting composition and melting points of multi-component molten salts, and also for ascertaining the other properties of molten salts, such as their densities and conductivities. It is expected to a quick method for design and selection of PCM for the high temperature latent heat energy storage systems, and also for other system adopted molten salt. It should be noted that ANN method is based on large number of samples with known data to predict the properties of unknown samples with similar structure, if the literature data of samples with similar structure is insufficient or inaccurate, the prediction accuracy will be discounted.

## Declaration of Competing Interest

All authors of this manuscript have directly participated in planning, execution, and/or analysis of this study. The contents of this manuscript have not been copyrighted or published previously. The contents of this manuscript are also not now under consideration for publication elsewhere. I am one author signing on behalf of all co-authors of this manuscript, and attesting to the above.

## Acknowledgements

Supported by National Key R&D Program of China (2018YFB1501002), Qinghai Major Science and Technology Projects (2017-GX-A3), “Transformational Technologies for Clean Energy and Demonstration”, Strategic Priority Research Program of the Chinese Academy of Sciences (Grant No. XDA21080000), K.C. Wong Education Foundation (Grant No. GJTD-2018-10).

## Appendix A. Supplementary material

Supplementary data to this article can be found online at <https://doi.org/10.1016/j.solener.2020.05.029>.

## References

- Chartrand, P., Pelton, A., 2001. Thermodynamic evaluation and optimization of the Li, Na, K, Mg, Ca//F, Cl reciprocal system using the modified quasi-chemical model. *Metall. Mater. Trans. A* 32 (6), 1417–1430.
- Cheng, X., Zhai, X., 2018. Thermal performance analysis and optimization of a cascaded packed bed cool thermal energy storage unit using multiple phase change materials. *Appl. Energy* 215, 566–576.
- Coley, W., Thomas, A., Lummiss, M., Jaworski, N., Breen, P., Schultz, V., Hart, T., Fishman, S., Rogers, L., Gao, H., Hicklin, W., Plehiers, P., Byington, J., Piotti, S., Green, H., Hart, J., Jamison, F., Jensen, F., 2019. A robotic platform for flow synthesis of organic compounds informed by AI planning. *Science* 365 (6453), eaax1566.
- Elfeky, E., Li, X., Ahmed, N., Lu, L., Wang, Q., 2019. Optimization of thermal performance in thermocline tank thermal energy storage system with the multilayered PCM(s) for CSP tower plants. *Appl. Energy* 243, 175–190.
- Fernández, G., Gomez-Vidal, J., Oró, E., Kruiuzenga, A., Solé, A., Cabeza, F., 2019. Mainstreaming commercial CSP systems: A technology review. *Renew. Energy* 140, 152–176.
- Gadzuric, S., Suh, C., Gaune-Escard, M., Rajan, K., 2006. Extracting information from the molten salt database. *Metall. Mater. Trans. A* 37 (12), 3411–3414.
- Garkushin, I., Sukhareenko, M., Ragrina, M., 2017. Cutting triangle NaF-KF-CsCl of the quaternary reciprocal system Na,K,Cs||F,Cl. *Russ. J. Inorg. Chem.* 62 (12), 1652–1658.
- Herrmann, U., Kearney, W., 2002. Survey of thermal energy storage for parabolic trough power plants. *J. Sol. Energy-T. Asme* 124 (2), 145.
- Hoshino, Y., Utsunomiya, T., Abe, O., 1981. The thermal decomposition of sodium nitrate and the effects of several oxides on the decomposition. *B. Chem. Soc. Jpn.* 54 (5), 1385–1391.
- Isayev, O., Oses, C., Toher, C., Gossett, E., Curtarolo, S., Tropsha, A., 2017. Universal fragment descriptors for predicting properties of inorganic crystals. *Nat. Commun.* 8 (1), 15679.
- Janz, J., Tomkins, T., Allen, B., 1979. Molten salts: Volume 4, Part 4 mixed halide melts electrical conductance, density, viscosity, and surface tension data. *J. Phys. Chem. Ref. Dat.* 8 (1), 125–302.
- Jiang, Y., Sun, Y., Jacob, D., Bruno, F., Li, S., 2018. Novel Na<sub>2</sub>SO<sub>4</sub>-NaCl ceramic composites as high temperature phase change materials for solar thermal power plants (Part I). *Sol. Energy Mat. Sol.* 178, 74–83.
- Kenisarin, M., 2010. High-temperature phase change materials for thermal energy storage. *Renew. Sust. Energy Rev.* 14 (3), 955–970.
- Li, C., Li, Q., Li, Y., She, X., Cao, H., Zhang, P., Wang, L., Ding, Y., 2019. Heat transfer of composite phase change material modules containing a eutectic carbonate salt for medium and high temperature thermal energy storage applications. *Appl. Energy* 238, 1074–1083.
- Lin, Y., Alva, G., Fang, G., 2018. Review on thermal performances and applications of thermal energy storage systems with inorganic phase change materials. *Energy* 165, 685–708.
- Liu, Y., Ji, X., Li, M., Kang, J., Zhang, J., Lu, W., 2016. Predicting the curie temperatures of La<sub>2</sub>M<sub>1-x-z</sub>R<sub>2</sub>Mn<sub>3</sub>N<sub>1-y</sub>O<sub>3</sub> perovskites based on support vector regression. *Comput. Appl. Chem.* 33 (6), 731–736.
- Malinovsky, M., Gregorčoková, J., 1974. The liquidus of sodium chloride in the system sodium chloride-calcium chloride. *Chem. Pap.-Chemicke Zvesti* 28 (4), 539–545.
- Mohan, G., Venkataraman, B., Coventry, J., 2019. Sensible energy storage options for concentrating solar power plants operating above 600 °C. *Renew. Sust. Energy Rev.* 107, 319–337.
- Myers, D., Goswami, Y., 2016. Thermal energy storage using chloride salts and their eutectics. *Appl. Therm. Eng.* 109 (Part B), 889–900.
- Navarrete, N., Mondragón, R., Wen, D., Navarro, E., Ding, Y., Juliá, E., 2019. Thermal energy storage of molten salt-based nanofluid containing nano-encapsulated metal alloy phase change materials. *Energy* 167, 912–920.
- Pelton, D., Talley, K., Sharma, A., 1992. Thermodynamic evaluation of phase equilibria in the CaCl<sub>2</sub>-MgCl<sub>2</sub>-CaF<sub>2</sub>-MgF<sub>2</sub> system. *J. Phase. Equilib.* 13 (4), 384–390.
- Reilly, E., Kolb, J., 2001. An Evaluation of Molten-Salt Power Towers Including Results of the Solar Two Project. Sandia National Laboratories, Albuquerque, NM, US and Livermore, CA US SAND2001-3674.
- Renaud, E., Robelin, C., Gheribi, E., Chartrand, P., 2011. Thermodynamic evaluation and optimization of the Li, Na, K, Mg, Ca, Sr//F, Cl reciprocal system. *J. Chem. Thermodyn.* 43 (8), 1286–1298.
- Sang, L., Li, F., Xu, Y., 2019. Form-stable ternary carbonates/MgO composite material for high temperature thermal energy storage. *Sol. Energy* 180, 1–7.
- Sharma, A., Johnson, I., 1969. Phase diagrams for the systems MgCl<sub>2</sub>-MgF<sub>2</sub>, CaCl<sub>2</sub>-MgF<sub>2</sub>, and NaCl-MgF<sub>2</sub>. *J. Am. Ceram. Soc.* 52 (11), 612–615.
- Songster, J., Pelton, D., 1991. Thermodynamic calculation of phase diagrams of the 60 common-ion ternary systems containing cations Li, Na, K, Rb, Cs and anions F, Cl, Br, I. *J. Phase Equilib.* 12 (5), 511–537.
- Stern, H., 1972. High temperature properties and decomposition of inorganic salts part 3, nitrates and nitrites. *J. Phys. Chem. Ref. Dat.* 1 (3), 747.
- Verdiev, N., Iskenderov, G., Arbukhanova, A., Amadziev, A., 2006. Three component system Na/F, Cl, Br. *Izvestiya VUZov. Severo-Kavkazskii Region. Nat. Sci.* 56–61 (in Russian).
- Verdiev, N., Arbukhanova, A., Iskenderov, G., 2009. NaF-NaBr-Na<sub>2</sub>MoO<sub>4</sub> and KF-KCl-KBr ternary systems. *Russ. J. Inorg. Chem.* 54 (1), 128–133.
- Xiao, X., Zhang, G., Ding, L., Wen, S., 2019. Rheological characteristics of molten salt seeded with Al<sub>2</sub>O<sub>3</sub> nanopowder and graphene for concentrated solar power. *Energies* 12 (3), 16.
- You, X., 1974. Polarizability of ions. *Chin. Sci. Bull.* 19 (9), 419–423 (in Chinese).
- Zeng, W., Guo, J., Chen, N., Guo, J., 1997. Computerized prediction of interaction parameters and phase diagrams of the immiscible binary systems of nontransition-nontransition metals. *Calphad* 21 (3), 289–293.
- Zhang, H., Shin, D., Santhanagopalan, S., 2019. Microencapsulated binary carbonate salt mixture in silica shell with enhanced effective heat capacity for high temperature latent heat storage. *Renew. Energy* 134, 1156–1162.
- Zhavoronkov, A., Ivanenkov, A., Aliper, A., Veselov, S., Aladinskiy, A., Aladinskaya, V., Terentiev, A., Polykovskiy, A., Kuznetsov, D., Asadulaev, A., Volkov, Y., Zholus, A., Shayakhmetov, R., Zhebrak, A., Minaeva, I., Zagribelnyy, A., Lee, H., Soll, R., Madge, D., Xing, L., Guo, T., Aspuru-Guzik, A., 2019. Deep learning enables rapid identification of potent DDR1 kinase inhibitors. *Nat. Biotechnol.* 37 (9), 1038–1040.
- Zhou, C., Wu, K., 2019. Medium- and high-temperature latent heat thermal energy storage: Material database, system review, and corrosivity assessment. *Int. J. Energy Res.* 43 (2), 621–661.
- Zhu, Q., Samanta, A., Li, B., Rudd, E., Frolov, T., 2018. Predicting phase behavior of grain boundaries with evolutionary search and machine learning. *Nat. Commun.* 9 (1), 467.
- Zou, Q., Jie, J., Shen, Z., Han, N., Li, T., 2019. A new concept of Al-Si alloy with core-shell structure as phase change materials for thermal energy storage. *Mater. Lett.* 237, 193–196.